International Journal of Mechanical, Industrial and Aerospace Sciences
ISSN: 2517-9950
Vol:5, No:1, 2011

# Numerical Analysis of Air Flow and Conjugated Heat Transfer in Internally Grooved Parallel-Plate Channels

Hossein Shokouhmand , Koohyar Vahidkhah, Mohammad A. Esmaeili

***Abstract*—**A numerical investigation of surface heat transfer characteristics of turbulent air flows in different parallel plate grooved channels is performed using CFD code. The results are obtained for Reynolds number ranging from 10,000 to 30,000 and for arc-shaped and rectangular grooved channels. The influence of different geometric parameters of dimples as well as the number of them and the geometric and thermophysical properties of channel walls are studied. It is found that there exists an optimum value for depth of dimples in which the largest wall heat flux can be achieved. Also, the results show a critical value for the ratio of wall thermal conductivity to the one of fluid in which the dependence of wall heat flux to this ratio almost vanishes. In most cases examined, heat transfer enhancement is larger for arc-shaped grooved channels than rectangular ones.

***Keywords*—**dimple, heat transfer enhancement, Numerical, optimum value, turbulent air flow.

## I. Introduction

ENHANCEMENT of the thermal performance of heat transfer devices is attempted in many engineering applications, such as compact heat exchangers, cooling systems for electronic equipments and nuclear reactor cores, as well as biomedical and aerospace applications. Numerical and experimental studies have shown that the heat transfer in dimpled channels is enhanced with respect to smooth ones, due to periodic interruptions of thermal boundary layers and also improvement in lateral mixing by disruption of the shear layer, separation of the bulk flow, formation of recirculating flow, and thus destabilization of the transversal vortices in the dimples. This enhancement is achieved with pressure drop penalties that are usually small when compared to other more invasive types of turbulence promoters.

There are abundant studies on fluid flows in the parallel plate channels with periodically dimpled parts. Also, there have been numerous investigations on heat transfer characteristics of such flows. Ghaddar et al. [1] numerically studied two dimensional incompressible isothermal cyclic flows in channels with integrated circuits protrusions. They found a critical value for the Reynolds number above which cyclic flow oscillations are observed. Ghaddar et al. [2] used two dimensional incompressible non-isothermal numerical simulations to show the possibility of improving heat transfer using the unsteadiness observed in their previous work. Amon and Mikic [3], and Amon [4] extended the studies in [1, 2] by investigating heat transfer enhancement for airflows above the critical value of Reynolds number.

Farhanieh et al. [5] numerically and experimentally investigated laminar fluid flow and heat transfer characteristics in a duct with a rectangular grooved wall. Their results indicated enhancement in the local Nusselt number compared with a smooth parallel plate duct due to re-establishment of thermal boundary layers and formation of recirculating flows inside the grooves. They also showed that this enhancement is accompanied by a relatively high pressure drop increase.

Bilen and Yapici [6] studied the effect of orientation angle of the turbulence promoters located on the channel wall on the heat transfer. They showed that the highest heat transfer rate is achieved when the promoter orientation angle is 45 degrees. Herman and Kang [7] investigated the heat transfer performance in grooved channels with curved vanes. Their results showed an increase in heat transfer by a factor of 1.5–3.5 due to increased flow velocities in the grooved region, when compared to the basic grooved channel. However, it was also found that there is a significant increase in the accompanying pressure drop penalty. Tanda [8] investigated the effect of rectangular and V-shaped ribs deployed transverse to the main flow direction with an angle of 45 or 60 degrees relative to it and also studied the effect of continuous and broken ribs. The effect of roughness with V-shaped ribs on the heat transfer and friction coefficient for both forward and backward flows in a rectangular channel was investigated by Chang et al. [9]. Wang and Sunden [10] investigated the heat transfer and friction characteristics in a square duct roughened by various-shaped transverse ribs on one wall.

Ridouane and Campo [11] numerically analyzed laminar air flows in parallel plate channels with hemi-cylindrical cavities on both walls using finite volume method. Their results showed that there exists an optimum value for the ratio of cavity depth to cavity print diameter in which the largest heat transfer rate from the wall is achieved.

Won and Ligrani [12] and Park et al. [13] numerically

F. H. Shokouhmand, Mech. Eng. Dep., University of Tehran, Tehran, Iran,
S. K. Vahidkhah, Med. Eng. Department, Amirkabir University of Technology (Tehran Polytechnic), Tehran, Iran (email: k.vahidkhah@gmail.com),
T. Mohammad A. Esmaeili, Mech. Eng. Dep., University of Tehran, Tehran, Iran (email: m.amin.esmaeili@gmail.com)

investigated the turbulent air flow in channels with dimples placed on the bottom wall using the $k-\varepsilon$ turbulence model under the platform of the commercial code FLUENT. Bilen et al. [14] experimentally studied the heat transfer and friction characteristics of fully developed turbulent airflows in grooved tubes with three different geometric groove shapes. Their results showed that the maximum heat transfer enhancement in comparison with smooth tubes is obtained for the tubes with circular grooves, then the ones with trapezoidal and finally with rectangular grooves.

Although plentiful studies have been accomplished in this field of research, but not many papers have been published to investigated the effect of channel wall thickness and its thermophysical properties on heat transfer characteristics. In this paper, conjugated heat transfer of air flow in parallel-plate grooved channels is numerically simulated and the influence of effective parameters, namely Reynolds number, geometric properties of channel and cavities, number of cavities, thickness of channel walls, and the effect of relative thermal conductivity of channel walls to the one of the fluid is investigated.

## II. Nomenclature

| | | |
|---|---|---|
| $c_p$ | [J/kgK] | Fluid specific heat |
| d | [m] | Horizontal deviation of upper wall cavities from the bottom wall ones (in staggered configuration) |
| $D_h$ | [m] | Hydraulic diameter |
| $E$ | [J] | Fluid total energy |
| $G_k$ | [kg/ms$^3$] | Generation of turbulence kinetic energy due to the mean velocity gradients |
| h | [m] | Depth of dimple |
| H | [m] | Height of channel |
| $k$ | [m$^2$/s$^2$] | Turbulence kinetic energy |
| $k_f$ | [W/mK] | Thermal conductivity of fluid |
| $k_w$ | [W/mK] | Thermal conductivity of channel wall |
| l | [m] | Dimple projection length |
| L | [m] | Distance between two subsequent dimples |
| $L_d$ | [m] | Exit length |
| $L_T$ | [m] | Length of channel |
| $L_u$ | [m] | Entrance length |
| $Nu$ | [-] | Nusselt number |
| $p$ | [Pa] | Fluid pressure |
| $Pr$ | [-] | Prandtl number |
| $q_w$ | [W/m$^2$] | Wall heat flux |
| $Re$ | [-] | Reynolds number |
| T | [m] | Channel wall thickness |
| $T_i$ | [K] | Fluid temperature at channel inlet |
| $T_w$ | [K] | Wall temperature |
| $u_i$ | [m/s] | Fluid velocity along $x_i$ |
| $\vec{v}$ | [m/s] | Velocity vector |
| $W$ | [m] | Channel width |
| $x_i$ | [m] | ith Cartesian axis direction |
| $\varepsilon$ | [m$^2$/s$^3$] | Turbulence kinetic energy dissipation rate |
| $\mu$ | [kg/ms] | Fluid viscosity |
| $\mu_t$ | [kg/ms] | Turbulent (or eddy) viscosity |
| $\rho$ | [kg/m$^3$] | Fluid density |
| $\sigma_k$ | [-] | Turbulent Prandtl number for $k$ |
| $\sigma_\varepsilon$ | [-] | Turbulent Prandtl number for $\varepsilon$ |

## III. Channel Geometry and Boundary Conditions

The channel under consideration is a two dimensional duct with a total length of $L_T$=34 cm and a height of H=2 cm. As can be seen in Fig. 1, the entrance and exit lengths are $L_u$= $L_d$=10 cm (so the middle part of the channel is the dimpled section with the length of 14 cm). The other geometric parameters are variants in different cases and configurations studied. The outer surfaces of channel walls are at constant temperature of 320 K and the inner ones are in coupled thermal interaction with the flowing air (heat is removed from these surfaces by forced convection due to the flowing air and it flows from outer surfaces to them by conduction in the solid wall). Turbulent incompressible air flow, with a density of 1.225 kg/m3, viscosity of 1.7894×10-5 kg/ms and specific heat of 1006.43 J/kgK, enters the duct in hydrodynamic fully developed condition (with parabolic velocity profile) at constant temperature of 280 K. At the outlet, the streamwise gradients of all variables are set to zero as an outflow boundary condition.

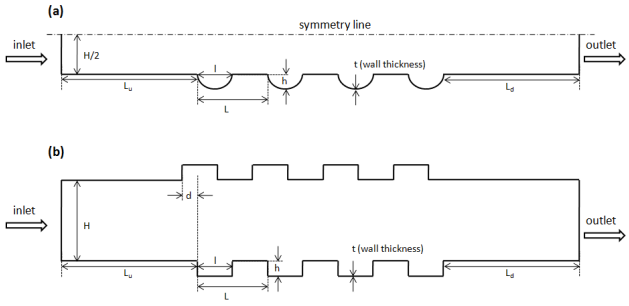


Fig. 1 Channel geometry (a) symmetric configuration with arc-shaped grooves, (b) staggered configuration with rectangular grooves

TABLE I
EFFECTIVE PARAMETERS

| Parameter | Definition | Values |
|---|---|---|
| h/H | the ratio of cavity height to channel height | H=20 mm, h=0,2,2.5,3,3.5,4,4.5,5,6 mm |
| l/L | the ratio of cavity projection length to the distance between two subsequent cavities | L=4 cm, l=0.5,1,1.5,2 cm |
| d/l | the ratio of horizontal deviation of upper wall cavities from bottom wall ones to the cavity projection length | l=2 cm, d=0,0.5,1,1.5,2 cm |
| t/H | the ratio of channel walls thickness to channel height | H=20 mm, t=0,0.3,0.5,0.7,1 mm |
| kw/kf | the ratio of thermal conductivity of channel walls to the one of the fluid | kf=0.0242 w/mK, kw=2.02, 6.07, 14.17, 25.3, 50.6, 101.2, 151.8, 202.4, 404.8 w/mK |
| N | the number of cavities | N=4, 7, 10, 13 |

As it is shown in Fig. 1, two configurations for dimpled channels are studied, one with symmetrically opposing cavities onto both walls and another with staggered cavities. In each configuration both rectangular and arc-shaped dimples are considered (in the case of arc-shaped grooves, each dimple is a part of a circle or an arc with projection length of l and depth of h). The effective parameters, that their influence on heat transfer enhancement is investigated in this paper, are listed in Table. I.

## IV. Governing Equations

The governing equations are the continuity, momentum, and energy equations. The flow is studied under the following assumptions: steady-state, constant fluid properties and no natural convection and body forces. With these assumptions continuity and momentum equations can be written as follows:

$$\nabla.(\rho\vec{v}) = 0 \tag{1}$$

$$\nabla.(\rho\vec{v}\vec{v}) = -\nabla p + \nabla.\left[\mu\left(\left(\nabla\vec{v} + \nabla\vec{v}^{T}\right) - \frac{2}{3}\nabla.\vec{v}I\right)\right] \tag{2}$$

The standard $k-\varepsilon$ model is used to simulate the turbulent fluid flow in the channel. This semi-empirical model is based on model transport equations for the turbulence kinetic energy, $k$, and its dissipation rate, $\varepsilon$, and is valid only for fully turbulent flows. $k$ and $\varepsilon$ are obtained from the following transport equations:

$$\frac{\partial}{\partial x_i}(\rho k u_i) = \frac{\partial}{\partial x_j}\left[\left(\mu + \frac{\mu_t}{\sigma_k}\right)\frac{\partial k}{\partial x_j}\right] + G_k - \rho\varepsilon \tag{3}$$

$$\frac{\partial}{\partial x_i}(\rho\varepsilon u_i) = \frac{\partial}{\partial x_j}\left[\left(\mu + \frac{\mu_t}{\sigma_\varepsilon}\right)\frac{\partial k}{\partial x_j}\right] + C_{1\varepsilon}\frac{\varepsilon}{k}G_k - C_{2\varepsilon}\rho\frac{\varepsilon^2}{k} \tag{4}$$

In these equations, $G_k$ represents the generation of turbulence kinetic energy due to the mean velocity gradients and $\mu_t$ the turbulent (or eddy) viscosity, is computed by combining $k$ and $\varepsilon$ in the equation $\mu_t = \rho C_\mu k^2/\varepsilon$. $C_{1\varepsilon}$ and $C_{2\varepsilon}$ are constants. $\sigma_k$ and $\sigma_\varepsilon$ are the turbulent Prandtl numbers for $k$ and $\varepsilon$, respectively. These model constants have been determined from experiments with air and water for fundamental turbulent shear flows:

$$C_{1\varepsilon} = 1.44,\ C_{2\varepsilon} = 1.92,\ C_\mu = 0.09,\ \sigma_k = 1.0,\ \sigma_\varepsilon = 1.3$$

Turbulent heat transport is modeled using the concept of Reynolds' analogy to turbulent momentum transfer. The "modeled" energy equation is thus given by the following:

$$\begin{aligned}&\frac{\partial}{\partial t}(\rho E) + \frac{\partial}{\partial x_i}\left[u_i(\rho E + p)\right] \\ &= \frac{\partial}{\partial x_j}\left[\left(k_f + \frac{c_p\mu_t}{\mathrm{Pr}_t}\right)\frac{\partial T}{\partial x_j}\right. \\ &\left. + u_i\left(\mu_{eff}\left(\frac{\partial u_j}{\partial x_i} + \frac{\partial u_i}{\partial x_j}\right) - \frac{2}{3}\mu_{eff}\frac{\partial u_i}{\partial x_i}\delta_{ij}\right)\right]\end{aligned} \tag{5}$$

Where $E$ is the total energy and the term that is multiplied by the temperature gradient term is called effective thermal conductivity.

## V. Numerical Method

The commercially available computational package, FLUENT, is used for the numerical model. In this software, the partial differential equations governing the problem are reduced to a system of algebraic equations using finite volume procedure. The discretization of the convective and diffusive fluxes across the control surfaces is modelled using the QUICK scheme and the pressure–velocity coupling is handled with the SIMPLE scheme.

Quad cells are used to mesh the problem domain and the grid points are distributed in a non-uniform manner with a higher concentration near the walls due to higher variable gradients expected in these locations.

To study the effect of grid fineness on the solution, the process of mesh refinement is repeated progressively until insignificant changes in the field variables happen.

## VI. Validation of Numerical Model

The numerical model is validated by simulating forced convection heat transfer in fully developed turbulent flow in smooth circular tubes and comparing the results for Nusselt number with correlation of Dittus-Boelter [15]. The result is shown in Fig. 2. The Dittus-Boelter correlation is described by the following equation:

$$Nu_D = 0.023\,\mathrm{Re}^{0.8}\,\mathrm{Pr}^{0.4} \tag{6}$$

In this equation $Nu_D$ and Re are computed as follows:

$$Nu_D = \frac{q_w}{(T_w - T_i)}\left(\frac{D_h}{k_f}\right) \quad , \quad \mathrm{Re} = \frac{\rho\bar{V}D_h}{\mu} \tag{7}$$

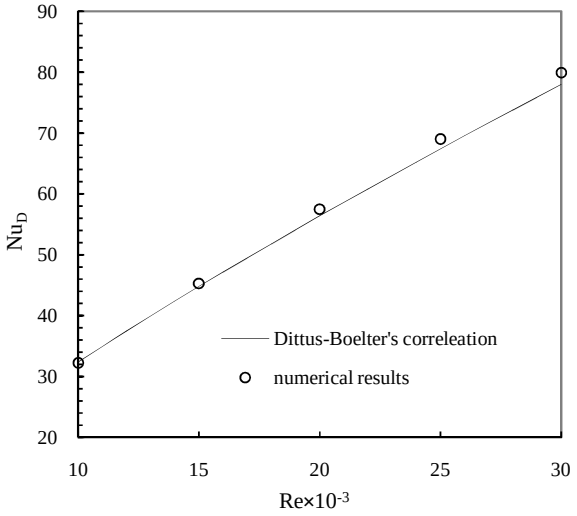


Fig. 2 Comparison between numerical predictions and empirical correlation for Nu as a function of Re in smooth circular tubes with turbulent fully developed fluid flow

Where $q_w$ is the wall heat flux at the thermal fully developed zone, $T_w$ is wall surface temperature, $T_i$ is the temperature of the inlet fluid, and $\bar{V}$ is the mean velocity of the fluid at the inlet. In the case of circular tube $D_h$ is equal to tube diameter, whereas for the case of parallel plate channel we have $D_h = 4A/P = 2HW/(H+W)$, where $W$ is the depth of channel which is assumed to be unity in this study because of the two dimensional problem. Good agreement that can be seen between numerical results and the empirical correlation in Fig. 2 ensures the validation of the numerical model for the study of different configurations of parallel plate grooved channels.

## VII. Results And Discussion

Flow patterns and heat transfer characteristics have been investigated numerically for different configurations mentioned in Fig. 1.

The streamlines and temperature distribution through the domain are presented for two sample symmetric cases in Fig. 3. In these two cases there are four cavities in the dimpled section of the channel with these geometric characteristics: l/L=0.5, h/H=0.15, and t/H=d/l=0. The Reynolds number is equal to 10,000 and the channel has arc-shaped dimples in the first case and rectangular ones in the second case. The effect of recirculation and vortices formed in the cavities on the temperature contours that causes heat transfer enhancement is clearly observed in this figure. Also it can be seen that in the second case (rectangular cavities) two clockwise vortices are formed in each dimple on the bottom wall, whereas in the first case (arc-shaped cavities) there is only one in each dimple.

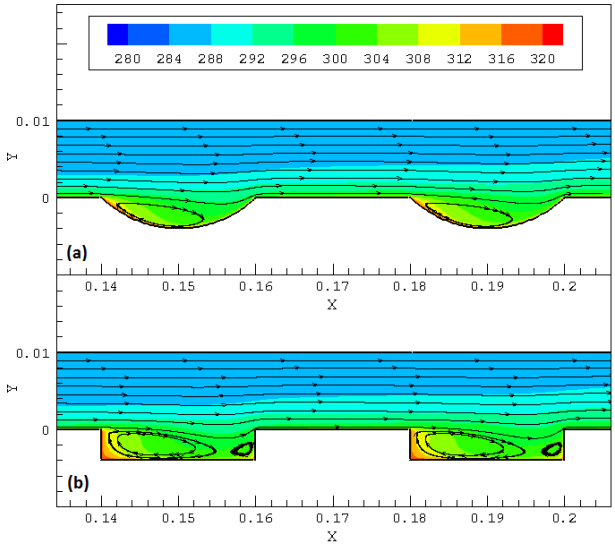


Fig. 3 streamlines and temperature distribution for two sample cases with N=4, Re=10,000, l/L=0.5, h/H=0.15, and t/H=d/l=0: (a) arc-shaped grooves, (b) rectangular grooves

Fig. 4 illustrates the variations of the mean Nusselt number as a function of Reynolds number for three different channel configurations; First with arc-shaped grooves, second with rectangular ones, and third without dimples (smooth channel). In all these cases we have symmetric channels with four cavities in dimpled section and l/L=0.5, h/H=0.15, and t/H=d/l=0. This figure shows that the mean Nusselt number increases as the Reynolds number increases.

The mean Nusselt number is obtained from (7) but one should substitute $q_w$ in this equation with mean wall heat flux which can be computed by integrating $q_w$ along the wall and dividing the value of integration by the length of the channel wall (including the length of cavities).

The effect of heat transfer conjugation is illustrated in Fig. 5. This figure shows the variations of wall heat flux with the ratio of thermal conductivity of channel walls to the one of the flowing fluid for four different cases with N=4, Re=10,000, l/L=0.5, h/H=0.15 and d/l=0. In the first two cases dimples are arc-shaped and in the second two they are rectangular. In each geometric condition two values for t/H is considered: 0.025 and 0.050. As presented in this figure, when $k_w/k_f$ is smaller than 250 as it increases the wall heat flux significantly increases. Though when the ratio is larger than $10^3$ the steep of the plot becomes almost zero. This value can be regarded as a critical value for $k_w/k_f$ in which the dependence of wall heat flux to this ratio vanishes.

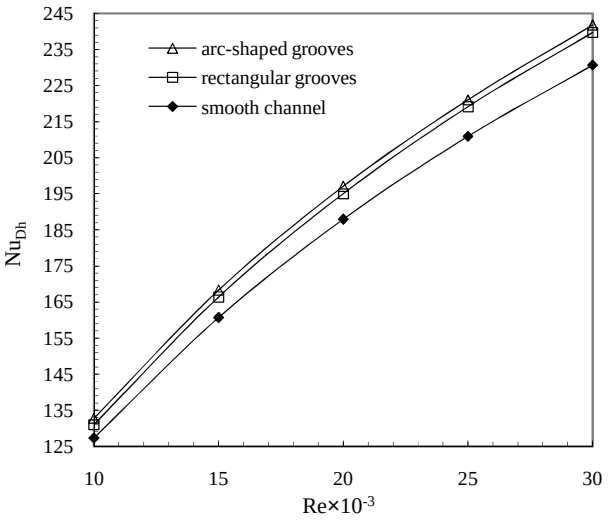


Fig. 4 Variations of the mean Nusselt number with the Reynolds number for three different cases with N=4, l/L=0.5, h/H=0.15, and t/H=d/l=0

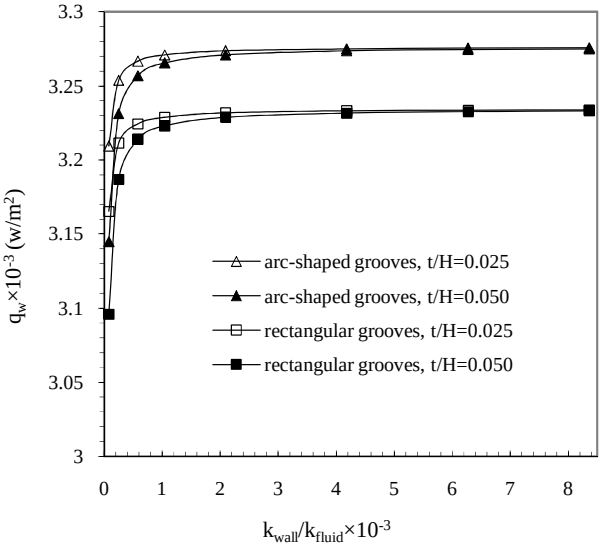


Fig. 5 Variations of the wall heat flux with the ratio of thermal conductivity of channel walls to the one of the fluid for four different cases with N=4, Re=10,000, l/L=0.5, h/H=0.15 and d/l=0

The variation of the wall heat flux as a function of l/L is

illustrated in Fig. 6 for four different symmetric cases. In all cases N=4, h/H=0.15 and t/H=d/l=0. As can be observed in Fig. 6 the heat transfer rate from the wall is slightly increased as l/L increases.

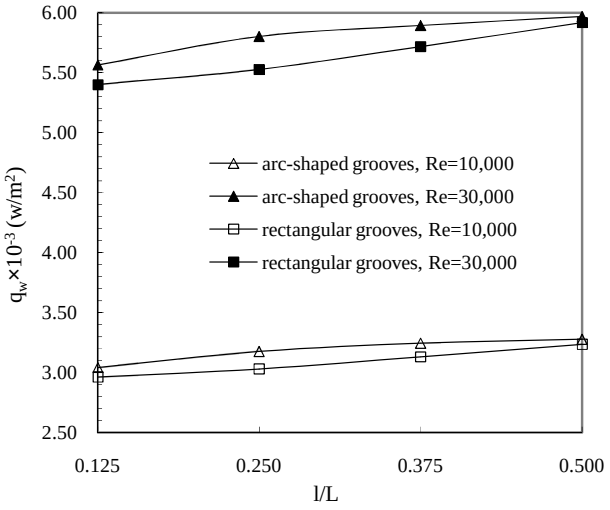


Fig. 6 Variations of wall heat flux with the ratio of cavity projection length to the distance between two subsequent cavities for four different cases with N=4, h/H=0.15 and t/H=d/l=0

The effect of variations in d/l and t/H on the wall heat flux was also investigated for arc-shaped and rectangular grooved channels with N=4, Re=10,000, h/H=0.15 and l/L=0.5. Since the effect of these two parameters in both cases turned out to be negligible the results are not presented here.

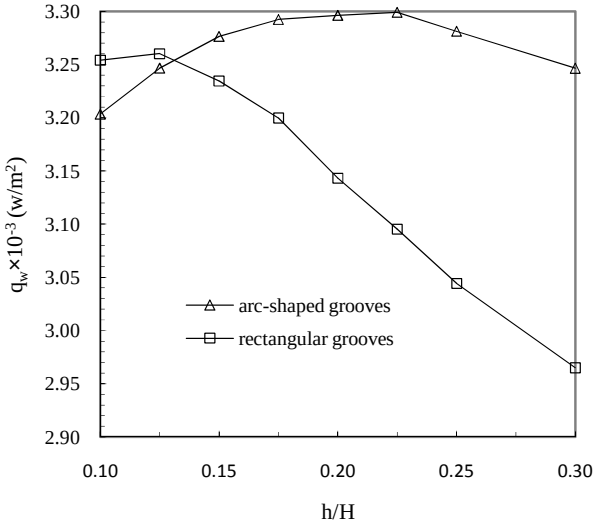


Fig. 7(a) Variation of wall heat flux with the ratio of dimples depth to the channel height. N=4, l/L=0.5, and t/H=d/l=0 and Re=10,000

Fig. 7(a) and Fig. 7(b) show the effect of dimple depth on heat transfer enhancement for two different Reynolds numbers. In all cases presented in these two figures N=4, l/L=0.5, and t/H=d/l=0. Same trends are observed in the figures for the two different Reynolds numbers. Also, it is obvious that there exists an optimum value for h/H in which the largest wall heat flux can be achieved. For both Reynolds numbers this optimum value for rectangular dimples is 0.125 and for arc-shaped dimples is 0.225. It is also observed that for lower values of h/H (smaller than 0.13) the rectangular dimples are more efficient than the arc-shaped ones but at larger values of h/H arc-shaped cavities show better enhancement in heat transfer.

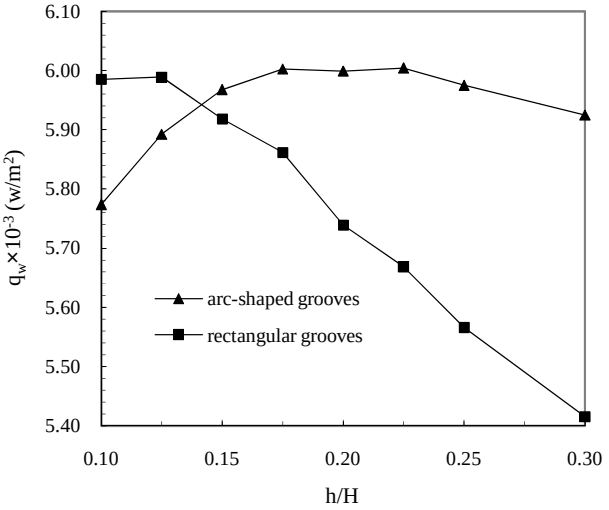


Fig. 7(b) Variation of wall heat flux with the ratio of dimples depth to the channel height. N=4, l/L=0.5, and t/H=d/l=0 and Re=30,000

Fig. 8 illustrates the variation of the wall heat flux with the number of dimples for four different cases. These cases are the same as the ones presented in Fig. 6 and in all of them h/H=0.15,l/L=0.125, t/H=d/l=0. The dimples have the same geometry and the number of them is increased while the channel has a constant length of dimpled section. This figure shows that the heat transfer rate from the channel wall is decreased as the number of cavities increases.

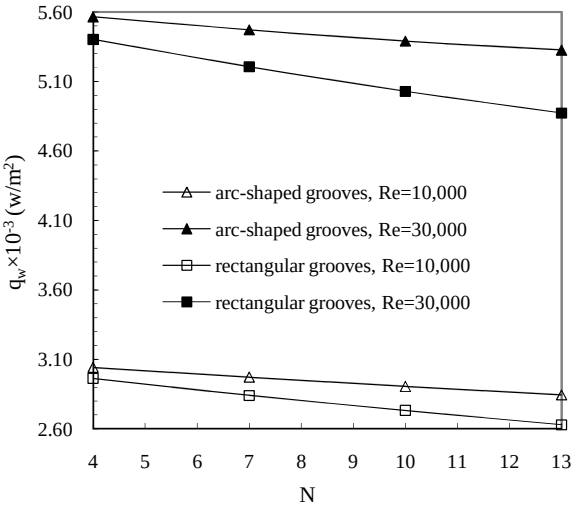


Fig. 8 Variation of the wall heat flux with the number of dimples for four different cases with h/H=0.15,l/L=0.125, t/H=d/l=0

## VIII. Conclusion

The effects geometric properties and number of dimples as well as thermophysical properties of channel wall on heat transfer enhancement in turbulent air flow in parallel plate channels were numerically investigated. The results of the present study can be summarized as follows:

1) The mean Nusselt number increases as the Reynolds number increases and at equal Reynolds numbers, generally arc-shaped grooved channels have larger values of mean Nu with respect to rectangular ones and as expected, the mean Nusselt number for both dimpled channels is larger than the one of smooth ducts.
2) The wall heat flux significantly increases as the ratio of wall thermal conductivity to the one of the fluid increases when this ratio is smaller than 250. Though at larger values of this ratio, namely 103 and higher, the dependence of wall heat flux to the ratio is negligible.
3) The effects of geometric parameters d/l, t/H, and l/L on heat transfer enhancement are negligible. Although, according to the results one can states that wall heat flux slightly increases as l/L or d/l increases and decreases trivially as t/H increases.
4) There exists an optimum value for h/H in which the highest heat transfer enhancement can be achieved. Also, for lower values of h/H the rectangular dimples are more efficient than the arc-shaped ones but at larger values of h/H arc-shaped cavities are more efficient.

Wall heat flux decreases slightly as the number of dimples increases in the dimpled section of the channel while this length and geometry of the dimples are held constant.

## References

[1] Ghaddar, N.K., Karczak, K.Z., Mikic, B.B., Patera, A.T., Numerical investigation of incompressible flow in grooved channels, Part 1. Stability and self-sustained oscillations, J. Fluid Mech.,163, 1986, pp. 99-127.
[2] Ghaddar, N.K., Megan, M., Mikic, B.B., Patera, A.T., Numerical investigation of incompressible flow in grooved channels, Part 2. Resonance and oscillatory heat-transfer enhancement, J. Fluid Mech.,168, 1986, pp. 541–567.
[3] Amon, C.H., Mikic, B.B., Numerical prediction of convective heat transfer in self-sustained oscillatory flows, J. Thermophys. Heat Transfer, Vol. 4, 1990, pp. 239-246.
[4] Amon, C.H., Heat transfer enhancement by flow destabilization in electronic chip configurations, J. Electron. Packag., Vol. 144, 1992, pp. 35-40.
[5] Fahanieh, B., Herman, C., Sunden B., Numerical and experimental analysis of laminar fluid flow and forced convection heat transfer in a grooved duct, Int. J. Heat Mass Transfer, Vol. 36, 1993, pp. 1609-1617.
[6] Bilen, K., Yapici, S., Heat transfer from a surface fitted with rectangular blocks at different orientation angle, Int. J. Heat Mass Transfer, Vol. 38, 2002, pp. 649-655.
[7] Herman, C., Kang, E., Heat transfer enhancement in a grooved channel with curved vanes, Int. J. Heat Mass Transfer, Vol. 45, 2002, pp. 3741-3757.
[8] Tanda, T., Heat transfer in rectangular channels with transverse and V-shaped broken ribs, Int. J. Heat Mass Transfer, Vol. 47, No. 2, 2004, pp. 229-243.
[9] Chang, S.W., Liou, T.M., Chiang, K.F., Hong, G.F., Heat transfer and pressure drop in rectangular channel with compound roughness of V-shaped ribs and deepened scales, Int. J. Heat Mass Transfer, Vol. 51, 2008, pp. 52-67.
[10] Wang, L., Sunden, B., Experimental investigation of local heat transfer in a square duct with various-shaped ribs, Int. J. Heat Mass Transfer, Vol. 43, 2007, pp. 759-766.
[11] Ridouane, H., Campo, A., Heat transfer and pressure drop characteristics of laminar air flows moving in a parallel-plate channel with transverse hemi-cylindrical cavities, Int. J. Heat Mass Transfer, Vol. 50, 2007, pp. 3913-3924.
[12] Won, S.Y., Ligrani, P.M., Numerical predictions of flow structure and local Nusselt number ratios along and above dimpled surfaces with different dimple depths in a channel, Num. Heat Transfer, Vol. 46, 2004, pp. 549-570.
[13] Park, J., Desam, P.R., Ligrani, P.M., Numerical predictions of flow structure above a dimpled surface in a channel, Num. Heat Transfer, Vol. 45, 2004, pp. 1-20.
[14] Bilen, K., Cetin, M., Gul, H., Balta, T., The investigation of groove geometry effect on heat transfer for internally grooved tubes, Applied Thermal Engineering, Vol. 29, 2009, pp. 753-761.
[15] Incropera, F.P., De Witt, D.P., Fundamentals of Heat and Mass Transfer, fourth ed., Wiley, 1996.